JOURNAL OF GUIDANCE, CONTROL, AND DYNAMICS
Vol. 28, No. 6, November–December 2005

Fault-Tolerant Particle Filtering by Using Interacting Multiple Model-Based Rao–Blackwellization

Ilia Rapoport* and Yaakov Oshman†
Technion—Israel Institute of Technology, 32000 Haifa, Israel

The problem of fault-tolerant particle filtering of a highly nonlinear system with fault-prone scalar measurement channels is addressed, in which each measurement channel is characterized by an additive measurement error generated by a linear scalar hybrid system. Particle filtering is an emerging method that exploits the recent advances in computer technology by using simulation-based techniques to represent probability density functions in nonlinear, non-Gaussian systems. Because, in the system under investigation, the overall state vector includes both the main states of the system and the parameters of the measurement channels, its size can be prohibitively large for efficient application of ordinary particle filtering, due to the required number of particles. The Rao–Blackwellization technique is adopted, allowing to estimate just the main system states using a reduced-size set of particles. The parameters of each measurement channel are estimated by a separate interacting multiple model scalar filter. A numerical example is presented, where four fault-prone magnetometers are used to estimate both the attitude of a spacecraft and the fault parameters of the measurement channels. The new state estimator is compared with unscented Kalman filtering-based techniques. The results demonstrate the superiority of the proposed algorithm in terms of estimation accuracy.

I. Introduction

FAULT-TOLERANT filtering of nonlinear systems with fault-prone measurement channels draws much attention because 1) many critical operations such as aircraft landing or spacecraft pointing and rendezvous require very accurate estimates even in the presence of measurement faults and 2) the majority of practical systems is indeed nonlinear.

A sensor fault can usually be expressed as a sudden addition of noise (white or colored) to the sensor measurement. Thus, global positioning system (GPS) spoofing error takes, in general, the form of colored noise and appears suddenly whenever it is activated.[1] A similar behavior is exhibited by the multipath effect.[2] Magnetometer faults, which are caused by magnetic fields generated by spacecraft electronics and electromagnetic torquing coils, usually take the form of biases (Ref. 3, p. 251) and appear whenever the corresponding current starts. Rate gyro faults, caused by input accelerations if the gyro gimbals are not perfectly balanced, are usually also modeled as biases (Ref. 3, p. 198) and, therefore, appear whenever the spacecraft accelerates.

A popular approach to model such fault-prone behavior is by means of hybrid systems or systems with switching parameters.[4] One of the switching parameter values corresponds in these applications to the nominal system operation, whereas the others represent various fault situations.[1,5] In systems with several independent fault-prone sensors and fault-free main dynamics, such as spacecraft, this general model can be simplified: The faults in different measurement channels can be modeled as separate Markovian Bernoulli random processes, where 1 designates a fault situation and 0 designates a nominal (fault-free) situation in the particular channel.

It is well-known that closed-form solutions for the optimal filtering problem exist only for a very narrow class of systems, for example, the Kalman filter (KF) for linear systems driven by Gaussian noises (continuous or discrete time) and the Wonham filter (see Ref. 6) for continuous-time hybrid linear systems the state vector of which is exactly measured. The optimal filtering algorithm for a general class of hybrid systems, whose dynamics as well as the measurement equations are linear with respect to the state vector, requires an exponentially growing bank of KFs[7] and is, therefore, impractical. A variety of suboptimal techniques were developed to prevent this growth.[4,8] The most popular due to its accuracy and simplicity, is the interacting multiple model (IMM) algorithm.[9] If the system dynamics is nonlinear, approximation techniques can be used, for example, extended KF (EKF) (see Ref. 10, p. 195) or unscented KF (UKF).[11]

Recent advances in computer technology gave rise to alternative methods of nonlinear Markovian system filtering, known as sequential Monte Carlo methods or particle filtering methods. Instead of estimating a finite number of the posterior distribution parameters, like the mean and covariance in the KF, the entire probability density function (PDF) is estimated. This posterior PDF is approximated by a set of particles, each of which represents some particular value of the system state vector. At each estimation cycle, these particles are propagated in time using the system dynamics equation and sampled values of the process noise. The measurement update is performed by calculating new relative weights of the particles using the measurement likelihood function (Ref.12, p. 10). As has been reported in, for example, Ref. 13, these Monte Carlo-based techniques exhibit clear accuracy and convergence-rate advantages over conventional closed-form suboptimal algorithms, such as the EKF or the UKF, in highly nonlinear systems.

In ordinary particle filtering, the larger the number of the particles, the more accurate is the estimate, due to the law of large numbers (Ref. 12, pp. 21–25). Therefore, the key requirement in particle filtering is to maintain a sufficiently large number of particles to represent adequately the posterior state distribution. This number grows exponentially with the state vector dimension. Low number of particles can cause degradation of the particle set and, consequentially, wrong state estimates. One technique for overcoming the problem is regularization of the particle set (Ref. 12, p. 251), which is equivalent to increasing the system process noise. When this method is used, the particle set degradation can be prevented; however, the estimate will no longer be optimal.

An alternative way to reduce the number of particles is to reduce the state vector dimension. This is possible, if, for example, the state vector can be partitioned into two sets, in which, given the history of

Received 6 June 2004; presented as Paper 2004-5416 at the AIAA Guidance, Navigation, and Control Conference, Providence, RI, 16–19 August 2004; revision received 28 February 2005; accepted for publication 12 March 2005.

*Ph.D. Student, Department of Aerospace Engineering.

†Professor, Department of Aerospace Engineering and Member, Asher Space Research Institute; yaakov.oshman@technion.ac.il. Associate Fellow AIAA.

one set, the other can be estimated in closed form using, for example, a KF. Thus, only the remaining part of the state vector has to be estimated using a particle set. Indeed, the number of computations per particle grows, but the total number of particles can be greatly reduced, thus reducing significantly the overall computational burden. This approach is known in the literature as Rao–Blackwellization (R–B) (see Ref. 12, p. 91).

In particular, this approach can be applied to hybrid systems, linear with respect to the state vector, as was done in Ref. 14. In that work, only the mode variable is evaluated using a particle set, whereas the state vector, conditioned on the mode, is produced by a linear Gaussian system and, therefore, is estimated using a KF. An extension to nonlinear hybrid systems was presented in Ref. 15. Similar to Ref. 14, the mode variable is evaluated using a particle set, whereas the state vector is estimated using a UKF.

The present work addresses the problem of filtering in highly nonlinear systems with independent scalar measurement channels. The additive measurement error in each channel is generated by a hybrid linear system with two possible modes (corresponding to the existence and nonexistence of a fault) and a single state variable. The nominal measurement noises are assumed to be Gaussian. Faulty measurement biases (possibly changing their values each time they appear) or faulty measurement noises (either white or colored) are examples of such a system. It is well known that, although an optimal closed-form estimation algorithm for linear hybrid systems does not exist, the IMM algorithm provides a good approximation of the optimal estimate. Therefore, it is proposed to apply the R–B technique. The distribution of the main state vector, representing the system dynamics, is approximated by a set of particles and estimated using a particle filter (PF). The estimates of the measurement channel parameters are obtained for each one of the particles by applying the IMM algorithm separately for each channel. Because of the separate handling of the channels and the fact that the dynamics of each measurement channel is scalar, the computational complexity per particle increases only by about 50–100%. The number of particles, on the other hand, can be greatly reduced, when compared to the ordinary PF, resulting in a significant overall computation saving.

The rest of the paper is organized as follows. The main principles of particle filtering and the R–B technique are reviewed in Sec. II. The estimation problem under consideration is formulated in Sec. III. The proposed estimation algorithm is then derived in Sec. IV. A numerical study illustrating the superiority of the proposed algorithm over UKF-based techniques is presented in Sec. V. Several concluding remarks are offered in the last section. For presentation clarity, the notational convention of Ref. 16 is adopted, according to which lower case and upper case letters are used to denote random variables and their realizations, respectively.

II. Particle Filtering Review

Main Principles

Consider the following nonlinear Markovian system

$$z_{k+1} = f_{k+1}(z_k, w_{k+1}) \tag{1}$$

with the following measurements:

$$y_k = h_k(z_k, v_k) \tag{2}$$

where z_k is the system state vector, $\{w_k\}_{k=1}^{\infty}$ is the process noise, and $\{v_k\}_{k=1}^{\infty}$ is the measurement noise. Both noise processes are assumed to be white and mutually independent. No Gaussian assumption is made. Let $\mathscr{Y}_k$ denote the measurement time history, namely,

$$\mathscr{Y}_k \triangleq \left[y_1^T, y_2^T, \ldots, y_k^T\right]^T \tag{3}$$

At each time step k the a posteriori state distribution $z_k | \mathscr{Y}_k$ is represented using a set of particles $\{Z_k(j)\}_{j=1}^N$ with associated weights $\{\lambda_k(j)\}_{j=1}^N$ satisfying

$$\sum_{j=1}^N \lambda_k(j) = N, \qquad \lambda_k(j) \geqslant 0 \quad \forall j \tag{4}$$

such that the posterior PDF is approximated as

$$p_{z_k|\mathscr{Y}_k}(Z_k|\Upsilon_k) \approx \frac{1}{N}\sum_{j=1}^N \lambda_k(j)\delta(Z_k - Z_k(j)) \tag{5}$$

where $\delta(\cdot)$ is Dirac's delta. The approximation (5) is in the integral sense, that is,

$$\int_{\mathscr{S}} g(Z_k) p_{z_k|\mathscr{Y}_k}(Z_k|\Upsilon_k)\, \mathrm{d}Z_k \approx \int_{\mathscr{S}} g(Z_k)\frac{1}{N}\sum_{j=1}^N \lambda_k(j)\delta(Z_k - Z_k(j))\, \mathrm{d}Z_k \qquad \forall \mathscr{S}, \quad \forall g(\cdot) \tag{6}$$

The particle filtering procedure comprises two steps: time propagation and measurement update (Ref. 12, p. 10). At the time propagation step, N values of the process noise w_{k+1} are sampled from its distribution, and each one of the particles evolves according to Eq. (1) using the sampled noise values. At the measurement update step, the particle weights are modified in the following way:

$$\lambda_{k+1}(j) = p_{y_{k+1}|z_{k+1}}(Y_{k+1}|Z_{k+1}(j))\lambda_k(j) \tag{7}$$

and then normalized such that condition (4) is satisfied. The likelihood function $p_{y_{k+1}|z_{k+1}}$ is derived from the measurement equation (2) and evaluated at the value of the current measurement Y_{k+1} and each one of the particles $Z_{k+1}(j)$.

One can see that the time-propagation step is simply a pure simulation of the system dynamics. The principle underlying the measurement update step of Eq. (7) is the Bayes law. Because

$$p_{z_{k+1}|\mathscr{Y}_{k+1}}(Z_{k+1}|\Upsilon_{k+1}) = \frac{p_{y_{k+1}|z_{k+1}}(Y_{k+1}|Z_{k+1})}{p_{y_{k+1}|\mathscr{Y}_k}(Y_{k+1}|\Upsilon_k)} p_{z_{k+1}|\mathscr{Y}_k}(Z_{k+1}|\Upsilon_k) \tag{8}$$

using approximation (5) for the $z_{k+1}|\mathscr{Y}_k$ distribution results in the following approximation for the $z_{k+1}|\mathscr{Y}_{k+1}$ distribution:

$$\begin{aligned} p_{z_{k+1}|\mathscr{Y}_{k+1}}(Z_{k+1}|\Upsilon_{k+1}) &\approx \frac{p_{y_{k+1}|z_{k+1}}(Y_{k+1}|Z_{k+1})}{p_{y_{k+1}|\mathscr{Y}_k}(Y_{k+1}|\Upsilon_k)}\frac{1}{N}\sum_{j=1}^N \lambda_k(j)\delta(Z_{k+1} - Z_{k+1}(j)) \\ &= \frac{1}{N p_{y_{k+1}|\mathscr{Y}_k}(Y_{k+1}|\Upsilon_k)}\sum_{j=1}^N [p_{y_{k+1}|z_{k+1}}(Y_{k+1}|Z_{k+1}(j))\lambda_k(j)] \\ &\quad \times \delta(Z_{k+1} - Z_{k+1}(j)) \end{aligned} \tag{9}$$

When managed in such a way, the particle set usually tends to degenerate because the weights of a relatively small particle subset, which is close enough to the true state, grow while the weights of the rest vanish. To prevent this tendency, a resampling technique is applied (Ref. 12, pp. 10 and 28). Each of the high-weighted particles is multiplied into several particles with smaller weights, whereas the low-weighted particles are deleted. As a result, a rich set of particles, distributed in the vicinity of the true state, is obtained. These particles, which have almost the same weights, constitute a correct approximation for the posterior state distribution.

Another problem, which usually arises in high-dimensional systems or systems with low process noise, is that after several resampling steps the particle set degenerates into a small number of subsets with identical particles. This renders the resulting particle distribution a discrete one. One possible method for preventing this phenomenon is by performing the regularization procedure (Ref. 12, p. 251), which is equivalent to increasing the system process noise.

R–B Concept

The R–B technique (see Ref. 12, p. 91) can be applied to systems whose state vector z_k can be partitioned as

$$z_k = \begin{bmatrix} z_k^{(1)} \\ z_k^{(2)} \end{bmatrix} \tag{10}$$

so that the distribution of $z_k^{(1)}$ given the measurement history $\mathscr{Y}_k$ and the history of the remaining states $z_k^{(2)}$ can be evaluated analytically. If, for example, the states $z_k^{(1)}$ together with the measurements y_k, given the history of $z_k^{(2)}$, behave as in a linear Gaussian system, then a KF can be used to estimate these states.

In this case, it is proposed to use a particle approximation only for the distribution of $z_k^{(2)} | \mathscr{Y}_k$. The distribution of $z_k^{(1)}$ conditioned on the measurements and on the history of $z_k^{(2)}$ is represented by a finite set of parameters that are required by the appropriate closed-form estimator. In the case of a KF, they are the mean and the covariance matrix. These parameters are handled separately for each one of the particles.

The entire estimation procedure consists of the following stages. At the time-propagation step, the particles $\{Z_k^{(2)}(j)\}_{j=1}^N$ evolve according to the following transitional distribution:

$$p_{z_{k+1}^{(2)}|z_k^{(2)},\ldots,\mathscr{Y}_k}\left(Z_{k+1}^{(2)}\middle|Z_k^{(2)},\ldots,\Upsilon_k\right) = \int_{-\infty}^{+\infty} p_{z_{k+1}^{(2)}|z_k^{(2)},z_k^{(1)}}\left(Z_{k+1}^{(2)}\middle|Z_k^{(2)},Z_k^{(1)}\right) \times p_{z_k^{(1)}|z_k^{(2)},\ldots,\mathscr{Y}_k}\left(Z_k^{(1)}\middle|Z_k^{(2)},\ldots,\Upsilon_k\right) \mathrm{d}Z_k^{(1)} \tag{11}$$

using the posterior distribution of $z_k^{(1)}$. The parameters of the $z_k^{(1)}$ distribution are then modified for each one of the particles according to the particular closed-form estimation algorithm used. At the measurement update step, the particle weights are modified using the likelihood function

$$p_{y_{k+1}|z_{k+1}^{(2)},z_k^{(2)},\ldots,\mathscr{Y}_k}\left(Y_{k+1}\middle|Z_{k+1}^{(2)},Z_k^{(2)},\ldots,\Upsilon_k\right) = \int_{-\infty}^{+\infty} p_{y_{k+1}|z_{k+1}^{(2)},z_{k+1}^{(1)}}\left(Y_{k+1}\middle|Z_{k+1}^{(2)},Z_{k+1}^{(1)}\right) \times p_{z_{k+1}^{(1)}|z_{k+1}^{(2)},z_k^{(2)},\ldots,\mathscr{Y}_k}\left(Z_{k+1}^{(1)}\middle|Z_{k+1}^{(2)},Z_k^{(2)},\ldots,\Upsilon_k\right)\mathrm{d}Z_{k+1}^{(1)} \tag{12}$$

which is computed using the parameters of the posterior distribution of $z_k^{(1)}$. Then, according to the closed-form algorithm, the measurement update is applied to the $z_k^{(1)}$ distribution parameters. Finally, resampling and regularization procedures are performed if deemed necessary. Notice that, by assumption, the conditional PDFs

$$p_{z_k^{(1)}|z_k^{(2)},\ldots,\mathscr{Y}_k}\left(Z_k^{(1)}\middle|Z_k^{(2)},\ldots,\Upsilon_k\right)$$
$$p_{z_{k+1}^{(1)}|z_{k+1}^{(2)},z_k^{(2)},\ldots,\mathscr{Y}_k}\left(Z_{k+1}^{(1)}\middle|Z_{k+1}^{(2)},Z_k^{(2)},\ldots,\Upsilon_k\right) \tag{13}$$

can be evaluated analytically. Therefore, both integrals in Eqs. (11) and (12) can also be computed analytically for each one of the sampled state histories.

Remark 1: The reason why this procedure provides correct results lies in the following remarkable fact. Assume that, for some time k, each one of the particles $Z_k^{(2)}(j)$ is replaced by its time history, that is, all of its values from time 0 to the time k. In this case, the resulting particle set represents the posterior distribution of the entire history of the true state, $p_{z_k^{(2)},z_{k-1}^{(2)},\ldots|\mathscr{Y}_k}(Z_k^{(2)}, Z_{k-1}^{(2)},\ldots|\Upsilon_k)$. To show this, notice the following identity:

$$\begin{aligned} p_{z_{k+1}^{(2)},z_k^{(2)},\ldots|\mathscr{Y}_{k+1}}\left(Z_{k+1}^{(2)},Z_k^{(2)},\ldots|\Upsilon_{k+1}\right) &= \frac{p_{y_{k+1}|z_{k+1}^{(2)},z_k^{(2)},\ldots,\mathscr{Y}_k}\left(Y_{k+1}\middle|Z_{k+1}^{(2)},Z_k^{(2)},\ldots,\Upsilon_k\right)}{p_{y_{k+1}|\mathscr{Y}_k}(Y_{k+1}|\Upsilon_k)} p_{z_{k+1}^{(2)},z_k^{(2)},\ldots|\mathscr{Y}_k}\left(Z_{k+1}^{(2)},Z_k^{(2)},\ldots\middle|\Upsilon_k\right) \\ &= \frac{\int_{-\infty}^{+\infty} p_{y_{k+1}|z_{k+1}^{(2)},z_{k+1}^{(1)}}\left(Y_{k+1}\middle|Z_{k+1}^{(2)},Z_{k+1}^{(1)}\right) p_{z_{k+1}^{(1)}|z_{k+1}^{(2)},z_k^{(2)},\ldots,\mathscr{Y}_k}\left(Z_{k+1}^{(1)}\middle|Z_{k+1}^{(2)},Z_k^{(2)},\ldots,\Upsilon_k\right)\mathrm{d}Z_{k+1}^{(1)}}{p_{y_{k+1}|\mathscr{Y}_k}(Y_{k+1}|\Upsilon_k)} \\ &\times \int_{-\infty}^{+\infty} p_{z_{k+1}^{(2)}|z_k^{(2)},z_k^{(1)}}\left(Z_{k+1}^{(2)}\middle|Z_k^{(2)},Z_k^{(1)}\right) p_{z_k^{(1)}|z_k^{(2)},\ldots,\mathscr{Y}_k}\left(Z_k^{(1)}\middle|Z_k^{(2)},\ldots,\Upsilon_k\right)\mathrm{d}Z_k^{(1)}\, p_{z_k^{(2)},z_{k-1}^{(2)},\ldots|\mathscr{Y}_k}\left(Z_k^{(2)},Z_{k-1}^{(2)},\ldots|\Upsilon_k\right) \end{aligned} \tag{14}$$

where the expression

$$\int_{-\infty}^{+\infty} p_{z_{k+1}^{(2)}|z_k^{(2)},z_k^{(1)}}\left(Z_{k+1}^{(2)}\middle|Z_k^{(2)},Z_k^{(1)}\right) \times p_{z_k^{(1)}|z_k^{(2)},\ldots,\mathscr{Y}_k}\left(Z_k^{(1)}\middle|Z_k^{(2)},\ldots,\Upsilon_k\right)\mathrm{d}Z_k^{(1)} \tag{15}$$

corresponds to the time propagation step [see Eq. (11)] and the expression

$$\frac{\int_{-\infty}^{+\infty} p_{y_{k+1}|z_{k+1}^{(2)},z_{k+1}^{(1)}}\left(Y_{k+1}\middle|Z_{k+1}^{(2)},Z_{k+1}^{(1)}\right) p_{z_{k+1}^{(1)}|z_{k+1}^{(2)},z_k^{(2)},\ldots,\mathscr{Y}_k}\left(Z_{k+1}^{(1)}\middle|Z_{k+1}^{(2)},Z_k^{(2)},\ldots,\Upsilon_k\right)\mathrm{d}Z_{k+1}^{(1)}}{p_{y_{k+1}|\mathscr{Y}_k}(Y_{k+1}|\Upsilon_k)} \tag{16}$$

corresponds to the measurement update step [see Eq. (12)]. Now, with use of the proposed algorithm, the PDFs (13) or, more precisely, their representing parameters, are computed correctly for each one of the particle time histories. Therefore, given a correct approximation of $p_{z_k^{(2)},z_{k-1}^{(2)},\ldots|\mathscr{Y}_k}(Z_k^{(2)}, Z_{k-1}^{(2)},\ldots|\Upsilon_k)$, the proposed estimation procedure yields a correct approximation for $p_{z_{k+1}^{(2)},z_k^{(2)},\ldots|\mathscr{Y}_{k+1}}(Z_{k+1}^{(2)}, Z_k^{(2)},\ldots|\Upsilon_{k+1})$.

III. Problem Formulation

The model discussed in this paper is a special case of the model defined by Eqs. (1) and (2). Consider the following nonlinear non-Gaussian state space model:

$$x_{k+1} = f_{k+1}(x_k, u_{k+1}, w_{k+1}), \qquad x \in \mathbb{R}^n \tag{17}$$

where $\{u_k\}_{k=1}^\infty$ is a sequence of (known) deterministic inputs, $\{w_k\}_{k=1}^\infty$ is a white sequence of the main process noise with known distribution (not necessarily Gaussian), and x_0 is the random initial state with known distribution. The system is measured through m independent channels, each of which generates scalar measurements and is potentially subject to a fault. The measurement equations are given by

$$y_k^{(i)} = h_k^{(i)}(x_k) + c_k^{(i)}(\gamma_k^{(i)})b_k^{(i)} + v_k^{(i)} \qquad i = 1, 2, \ldots, m \tag{18}$$

where $\{v_k^{(i)}\}_{k=1}^\infty$, $i = 1, 2, \ldots, m$, are independent Gaussian white sequences of measurement noises with $v_k^{(i)} \sim \mathscr{N}(0, R_k^{(i)}(\gamma_k^{(i)}))$ and $R_k^{(i)}(\gamma_k^{(i)}) > 0$; $\{\gamma_k^{(i)}\}_{k=1}^\infty$ is a Bernoulli Markov chain of fault indicators; and $b_k^{(i)}$ is a faulty measurement error. The distribution of the fault indicator sequence is described by the following initial and transition probabilities:

$$\Pr\left\{\gamma_0^{(i)} = 1\right\} = \Pi_0^{(i)} \tag{19a}$$

$$\Pr\left\{\gamma_{k+1}^{(i)} = \xi \middle| \gamma_k^{(i)} = \eta\right\} = P_{\xi\eta}^{(i)}(k+1|k) \qquad \xi, \eta \in \{0, 1\} \tag{19b}$$

The measurement error sequence $\{b_k^{(i)}\}_{k=1}^{\infty}$ is a scalar Markov process described by the following dynamics equation:

$$b_{k+1}^{(i)} = a_{k+1}^{(i)}\left(\gamma_{k+1}^{(i)}\right)b_k^{(i)} + g_{k+1}^{(i)}\left(\gamma_{k+1}^{(i)}\right)\tilde{w}_{k+1}^{(i)} \tag{20}$$

where $\{\tilde{w}_k^{(i)}\}_{k=1}^{\infty}$ are independent Gaussian white sequences, with $\tilde{w}_k^{(i)} \sim \mathcal{N}(0, q_k^{(i)})$. It is assumed that x_0, $\{w_k\}_{k=1}^{\infty}$, $\{\gamma_k^{(i)}\}_{k=0}^{\infty}$, $\{v_k^{(i)}\}_{k=1}^{\infty}$, $\{\tilde{w}_k^{(i)}\}_{k=1}^{\infty}$, and b_0 are mutually independent. In the sequel, the explicit time dependence of the parameters $P_{ij}^{(i)}(k+1|k)$, $c_k^{(i)}$, $R_k^{(i)}$, $a_k^{(i)}$, and $g_k^{(i)}$ is suppressed for notational simplicity.

The goal of this work is to derive an optimal minimum mean square error estimation algorithm for the states and fault indicators of the system.

The model addressed in this work can describe a wide class of fault-prone measurement systems. Thus, $a^{(i)}(\gamma) \equiv 1$, $g^{(i)}(\gamma) \equiv 0$, and $c^{(i)}(\gamma) \equiv 1$ correspond to a system with permanent measurement biases, whereas

$$a^{(i)}(\gamma) = c^{(i)}(\gamma) = \begin{cases} 0, & \text{for } \gamma = 0 \\ 1, & \text{for } \gamma = 1 \end{cases}, \qquad g^{(i)}(\gamma) = \begin{cases} 1, & \text{for } \gamma = 0 \\ 0, & \text{for } \gamma = 1 \end{cases} \tag{21}$$

correspond to a system with faulty measurement biases that change their value each time they appear, and $a^{(i)}(\gamma) \equiv 0$, $g^{(i)}(\gamma) \equiv 1$, and $c^{(i)}$ as in Eq. (21) yield a system with additive faulty white noises.

The following definition is used in the sequel:

$$y_k \triangleq \left[y_k^{(1)}, y_k^{(2)}, \ldots, y_k^{(m)}\right]^T \tag{22}$$

and the measurement history $\mathscr{Y}_k$ is still defined by Eq. (3).

IV. New Filtering Algorithm

Underlying Concept

The underlying idea is based on the fact that, according to Eqs. (18) and (20), the pairs $(b^{(i)}, \gamma^{(i)})$ are generated by independent linear hybrid systems, and given the history of the main state x, their measurements are also independent across different channels. It is well known that, although an optimal closed-form estimation algorithm for linear hybrid systems does not exist, the IMM algorithm[9] (detailed in the sequel) provides a good approximation of the optimal estimate.

The IMM estimator consists of a bank of KFs designed each for a different discrete mode of the system. The residuals produced by these filters are used to form the mode likelihood functions, which then serve in a hypothesis testing mechanism. The stage that makes the IMM algorithm particularly powerful is the interaction stage. During this stage, the estimates of all KFs in the bank are mixed using mixing probabilities such that the less likely estimates are "punished" in the sense that their covariance matrices grow relative to those of more likely modes.

With reliance on the IMM's well-known performance in hybrid systems, and based on the insight just mentioned, it is proposed to apply the R–B technique, in which at each time step k the distribution of the main state vector x_k is represented by a set of particles $\{X_k(j)\}_{j=1}^{N}$. Given the history of each particle $X_k(j)$, the posterior distribution of each pair $(b^{(i)}, \gamma^{(i)})$ can be estimated using the IMM algorithm. This computation is based on the $y_k^{(i)}$ measurement only, that is, on the measurement acquired by the same channel and not on measurements from other channels. Thus, each one of the IMM filters is applied to a scalar system, which renders the computations relatively simple.

According to the underlying principles of the IMM algorithm,[9] it is assumed that the distribution of

$$b_{k+1}^{(i)}, y_{k+1}^{(i)} \middle| \gamma_{k+1}^{(i)}, x_{k+1}, x_k, \ldots, \mathscr{Y}_k$$

is Gaussian. Therefore, for each particle $X_k(j)$, the posterior distribution of the pairs $(b^{(i)}, \gamma^{(i)})$ can be represented by the following quantities:

$$\hat{b}_{k|r,l}^{(i)}(\xi; j) \triangleq E\left[b_k \middle| \gamma_r^{(i)} = \xi, x = X_k(j), \mathscr{Y}_l\right], \qquad \xi = 0, 1 \tag{23a}$$

$$\hat{\pi}_{k|r,l}^{(i)}(\xi; j) \triangleq \operatorname{var}\left[b_k \middle| \gamma_r^{(i)} = \xi, x = X_k(j), \mathscr{Y}_l\right], \qquad \xi = 0, 1 \tag{23b}$$

$$\hat{\gamma}_{k|l}^{(i)}(j) \triangleq \Pr\left\{\gamma_k^{(i)} = 1 | x = X_k(j), \mathscr{Y}_l\right\} \tag{23c}$$

Remark 2: Note that the proposed approach, which approximates only the main state's posterior distribution by a particle set and estimates the fault parameters in closed form, is diametrically opposite to the approach taken in Ref. 15: There, a particle set is used for the fault mode parameters and a closed-form estimator is used for all other states. This role reversal is important because, unlike Ref. 15, no approximation is applied to the nonlinear part of the system in the proposed algorithm. Therefore, the resulting estimate can be expected to be more accurate than that of Ref. 15, though it is conceivable that it should be more computationally demanding.

Filtering Algorithm

The resulting filtering algorithm can be summarized as follows. At time k, the marginal distribution of $x_k | \mathscr{Y}_k$ is represented by the particle set $\{X_k(j)\}_{j=1}^{N}$. For each particle $X_k(j)$, the conditional distributions $b_k^{(i)}, \gamma_k^{(i)} | x_k, \mathscr{Y}_k$ are represented by the parameters $\hat{b}_{k|k,k}^{(i)}(\xi; j)$, $\hat{\pi}_{k|k,k}^{(i)}(\xi; j)$, $\hat{\gamma}_{k|k}^{(i)}(j)$. Then the steps of the algorithm are as follows.

1) Propagate the main state particles $\{X_k(j)\}_{j=1}^{N}$ one time step ahead, according to Eq. (17), for sampled values of the process noise w_{k+1}.

2) For each particle $X_{k+1}(j)$ and each measurement channel i, perform the time propagation and mixing steps of the IMM algorithm:

$$\hat{\gamma}_{k+1|k}^{(i)}(j) = P_{11}^{(i)}\hat{\gamma}_{k|k}^{(i)}(j) + P_{10}^{(i)}\left[1 - \hat{\gamma}_{k|k}^{(i)}(j)\right] \tag{24a}$$

$$\hat{b}_{k|k+1,k}^{(i)}(\xi; j) = \sum_{\eta=0}^{1} \mu_{\xi\eta}^{(i)}\hat{b}_{k|k,k}^{(i)}(\eta; j) \tag{24b}$$

$$\hat{\pi}_{k|k+1,k}^{(i)}(\xi; j) = \sum_{\eta=0}^{1} \mu_{\xi\eta}^{(i)}\left\{\hat{\pi}_{k|k,k}^{(i)}(\eta; j) + \left[\hat{b}_{k|k,k}^{(i)}(\eta; j) - \hat{b}_{k|k+1,k}^{(i)}(\xi; j)\right]^2\right\} \tag{24c}$$

$$\hat{b}_{k+1|k+1,k}^{(i)}(\xi; j) = a^{(i)}(\xi)\hat{b}_{k|k+1,k}^{(i)}(\xi; j) \tag{24d}$$

$$\hat{\pi}_{k+1|k+1,k}^{(i)}(\xi; j) = \left[a^{(i)}(\xi)\right]^2\hat{\pi}_{k|k+1,k}^{(i)}(\xi; j) + \left[g^{(i)}(\xi)\right]^2 q^{(i)} \tag{24e}$$

where

$$\mu_{\xi\eta}^{(i)} \triangleq P_{\xi\eta}^{(i)} \frac{\eta\hat{\gamma}_{k|k}^{(i)}(j) + (1-\eta)\left[1 - \hat{\gamma}_{k|k}^{(i)}(j)\right]}{\xi\hat{\gamma}_{k+1|k}^{(i)}(j) + (1-\xi)\left[1 - \hat{\gamma}_{k+1|k}^{(i)}(j)\right]} \tag{25}$$

and $P_{\xi\eta}^{(i)}$ is defined in Eq. (19b).

3) Update the particles' weights using Eq. (7) with the following likelihood function:

$$p_{y_{k+1}|x_{k+1},x_k,\ldots}(Y_{k+1}|X_{k+1}(j), \ldots) = \prod_{i=1}^{m} p_{y_{k+1}^{(i)}|x_{k+1},x_k,\ldots}\left(Y_{k+1}^{(i)} \middle| X_{k+1}(j), \ldots\right) \tag{26}$$

Each one of the PDF's $p_{y_{k+1}^{(i)}|x_{k+1},x_k,\ldots}[Y_{k+1}^{(i)}, X_{k+1}(j),\ldots]$ is computed using the time-propagated parameters, $\hat{b}_{k+1|k+1,k}^{(i)}(\xi; j)$, $\hat{\pi}_{k+1|k+1,k}^{(i)}(\xi; j)$ and $\hat{\gamma}_{k+1|k}^{(i)}(j)$, as follows:

$$p_{y_{k+1}^{(i)}|x_{k+1},x_k,\ldots}\left(Y_{k+1}^{(i)}, X_{k+1}(j),\ldots\right) = \hat{\gamma}_{k+1|k}^{(i)}(j) f_1^{(i)}(j) + \left[1 - \hat{\gamma}_{k+1|k}^{(i)}(j)\right] f_0^{(i)}(j) \tag{27}$$

where

$$f_\xi^{(i)}(j) \triangleq \left(1\Big/\sqrt{2\pi\sigma_\xi^2}\right) \exp\Big[-\left(1\big/2\sigma_\xi^2\right)\Big\{Y_{k+1}^{(i)} - h_k^{(i)}(X_k(j)) - c^{(i)}(\xi)\hat{b}_{k+1|k+1,k}^{(i)}(\xi; j)\Big\}^2\Big], \qquad \xi \in \{0, 1\} \tag{28}$$

$$\sigma_\xi^2 \triangleq \left[c^{(i)}(\xi)\right]^2 \hat{\pi}_{k+1|k+1,k}^{(i)}(\xi; j) + R^{(i)}, \qquad \xi \in \{0, 1\} \tag{29}$$

4) For each particle $X_{k+1}(j)$ and each measurement channel i, perform the measurement update step of the IMM algorithm,

$$K(\xi) = \frac{c^{(i)}(\xi)\hat{\pi}_{k+1|k+1,k}^{(i)}(\xi; j)}{\left[c^{(i)}(\xi)\right]^2 \hat{\pi}_{k+1|k+1,k}^{(i)}(\xi; j) + R^{(i)}} \tag{30a}$$

$$\tilde{Y}^{(i)}(\xi) = Y_{k+1}^{(i)} - h_k^{(i)}(X_{k+1}(j)) - c^{(i)}(\xi)\hat{b}_{k+1|k+1,k}^{(i)}(\xi; j) \tag{30b}$$

$$\hat{b}_{k+1|k+1,k+1}^{(i)}(\xi; j) = \hat{b}_{k+1|k+1,k}^{(i)}(\xi; j) + K(\xi)\tilde{Y}^{(i)}(\xi) \tag{30c}$$

$$\hat{\pi}_{k+1|k+1,k+1}^{(i)}(\xi; j) = \left[1 - K(\xi)c^{(i)}(\xi)\right]\hat{\pi}_{k+1|k+1,k}^{(i)}(\xi; j) \tag{30d}$$

$$\hat{\gamma}_{k+1|k+1}^{(i)}(j) = \frac{f_1^{(i)}(j)\hat{\gamma}_{k+1|k}^{(i)}(j)}{f_1^{(i)}(j)\hat{\gamma}_{k+1|k}^{(i)}(j) + f_0^{(i)}(j)\left[1 - \hat{\gamma}_{k+1|k}^{(i)}(j)\right]} \tag{30e}$$

where $f_\xi^{(i)}(j)$ are defined in Eq. (28).

5) Resample and regularize the particle set $\{X_{k+1}(j)\}_{j=1}^N$ according to predetermined criteria. (See, for example, Ref. 12, p. 232.)

For output purposes only the system state estimates can be obtained at any time step as weighted averages of the particle values, namely

$$\hat{x}_{k|k} = \frac{1}{N}\sum_{j=1}^{N} \lambda_k(j) X_k(j) \tag{31a}$$

$$\hat{b}_{k|k}^{(i)} = \frac{1}{N}\sum_{j=1}^{N} \lambda_k(j)\Big[\hat{b}_{k|k,k}^{(i)}(0; j)\left(1 - \hat{\gamma}_{k|k}^{(i)}(j)\right) + \hat{b}_{k|k,k}^{(i)}(1; j)\hat{\gamma}_{k|k}^{(i)}(j)\Big] \tag{31b}$$

$$\hat{\gamma}_{k|k}^{(i)} = \frac{1}{N}\sum_{j=1}^{N} \lambda_k(j)\hat{\gamma}_{k|k}^{(i)}(j) \tag{31c}$$

V. Simulation Study

A numerical simulation study has been carried out to demonstrate the superiority of the proposed algorithm over competing approaches. Specifically, two such approaches are examined: 1) the widely accepted approach to filtering in hybrid systems, namely, the IMM filter, and 2) the R–B approach proposed in Ref. 15, which is reversed relative to the approach proposed in this work. According to this approach, the fault parameters are estimated by a PF, whereas the continuously distributed states are estimated via a closed-form nonlinear estimator, for example, UKF. The results of this study are presented in this section.

System

In this study, the estimation of spacecraft attitude from vector observations of Earth's magnetic field is considered. Let q_k be the quaternion of rotation from a reference frame $\mathcal{R}$ to the spacecraft body frame $\mathcal{B}$. The quaternion is defined on the four-dimensional unit hypersphere and composed of vector and scalar parts, respectively,

$$q_k = \left[\varrho_k^T \quad q_{4k}\right]^T \tag{32}$$

The reference frame is associated with the spacecraft orbit: Its X axis is along the spacecraft path in its orbit, the Z axis is in the orbit plane and directed toward Earth, and the Y axis complies with the right-hand rule. The discrete-time dynamics equation of the rotating spacecraft is given by

$$q_{k+1} = \Phi_k(\omega_k) q_k \tag{33}$$

where the orthogonal matrix Φ_k is expressed using $\omega_k = [\omega_{1k}, \omega_{2k}, \omega_{3k}]^T$, the angular velocity vector of $\mathcal{B}$ with respect to $\mathcal{R}$ resolved in $\mathcal{B}$. Assuming that ω_k is constant during the sampling time interval Δt yields

$$\Phi_k(\omega_k) = \begin{bmatrix} -\frac{1}{2}[\omega_k\times]\Delta t & -\frac{1}{2}\omega_k\Delta t \\ -\frac{1}{2}\omega_k\Delta t & 0 \end{bmatrix} \tag{34}$$

where the cross-product matrix associated with the vector ω_k is defined as

$$[\omega_k\times] = \begin{bmatrix} 0 & -\omega_{3k} & \omega_{2k} \\ \omega_{3k} & 0 & -\omega_{1k} \\ -\omega_{2k} & \omega_{1k} & 0 \end{bmatrix} \tag{35}$$

The spacecraft is equipped with four magnetometers measuring Earth's magnetic field components in the $\mathcal{B}$ frame. The observation model is accordingly given by

$$y_k = HA(q_k)r_k + e_k, \qquad y_k \in \mathbb{R}^4 \tag{36}$$

where r_k is the precomputed value of Earth's magnetic field, given in the $\mathcal{R}$ frame, $A(q_k)$ is the rotation matrix (also known as the attitude matrix or direction cosine matrix) associated with the rotational quaternion q_k, H is the matrix of magnetometer directions, and e_k is the measurement error vector. One magnetometer is aligned along the spacecraft X axis, another is aligned along its Y axis, and the remaining two are aligned along the Z axis, that is,

$$H = \begin{bmatrix} 1 & 0 & 0 \\ 0 & 1 & 0 \\ 0 & 0 & 1 \\ 0 & 0 & 1 \end{bmatrix} \tag{37}$$

For simplicity, and without losing an essential characteristic of the example, it is assumed that the spacecraft angular rate ω_k is perfectly measured by the spacecraft rate gyros, so that the main system dynamics associated with Eq. (33) is noise free. Note that particle filtering of the attitude quaternion in the noisy gyros case has been treated in Ref. 13.

The fault-prone magnetometers suffer from measurement noise and suddenly appearing and disappearing measurement biases that change their values each time they appear [see Eq. (21)]. As has been mentioned earlier, such faulty behavior can be caused by spacecraft uncompensated electronics and electromagnetic torquing coils (Ref. 3, p. 251). More specifically, for every $i = 1, 2, 3, 4$,

$$e_k^{(i)} = \gamma_k^{(i)} b_k^{(i)} + v_k^{(i)}, \qquad v_k^{(i)} \sim \mathcal{N}\left(0, R^{(i)}\right) \tag{38a}$$

$$b_k^{(i)} = \gamma_k^{(i)} b_{k-1}^{(i)} + \left(1 - \gamma_k^{(i)}\right)\tilde{w}_k^{(i)}, \qquad \tilde{w}_k^{(i)} \sim \mathcal{N}\left(0, q^{(i)}\right) \tag{38b}$$

The Markovian Bernoulli fault sequences $\{\gamma_k^{(i)}\}_{k=1}^\infty$ are assumed to be generated by independent random telegraph processes with rates $\mu^{(i)}$. It is assumed that the measurements are acquired at a rate of 1 per every 10 time steps. The initial spacecraft attitude quaternion is assumed to be uniformly distributed over the unit four-dimensional sphere. The mathematical model's parameters are summarized in Table 1.

Comparison to Alternative Filtering Schemes

In this numerical study the proposed algorithm is compared to two alternative estimation schemes. The PF part of the proposed estimator is based on the recently proposed quaternion PF (QPF).[13] The particle set represents the posterior distribution of the attitude quaternion (four parameters). The effective state dimension in this

Table 1 Model parameters

Parameter	Value
$\mu^{(i)}$	0.001 1/s
$R^{(i)}$	50^2 nT^2
$\sqrt{(q^{(i)}/R^{(i)})}$	4
Orbit semimajor axis	6.7×10^6 m
Orbit eccentricity	0
Orbit inclination	35 deg
Δt	1 s

case is three due to the normalization constraint. The particle set is initialized with $N_{\text{init}} = 2000$ particles and then reduced to the $N = 300$ most likely particles. The reduction is performed when the effective sample size, given by

$$N_{\text{eff}} = (N_{\text{init}}) \bigg/ \frac{1}{N_{\text{init}}} \sum_{j=1}^{N_{\text{init}}} \lambda_k(j)^2 \tag{39}$$

drops below 300, where $\lambda_k(j)$ are the particle weights. Resampling and regularization are performed each time the effective sample size drops below $N_{\text{th}} = 100$ using the method described in Ref. 13. To prevent possible degeneracy of the particle set, the particles are reinitialized each time the likelihood value associated with the most likely particle drops below 10^{-8}. Obviously, every filter initialization is associated with short-termed large estimation errors. To eliminate these errors, a pure time propagation of the most recently available state estimate is implemented until the particle set is reduced again to 300 particles.

The auxiliary states (the fault parameters) are handled by separate IMM estimators, one per each measurement channel. The state vector in the IMM filter, designed for the ith measurement channel, is composed of a single state $b_k^{(i)}$, that is, of the measurement bias in this channel. The corresponding mode parameter is the fault indicator $\gamma_k^{(i)}$, which takes two values: 0 and 1. According to the number of measurements, one, thus, has to run four separate IMM filters, each having a single state and a binary mode, per particle, to implement the proposed filtering scheme.

The entire IMM-based R–B estimation scheme is termed, in the context of the present numerical study, RB–IMM/QPF.

Comparison to a Global IMM Filter

As mentioned earlier, a natural candidate filtering algorithm for hybrid systems, such as the system used in this example, is the IMM filter.[9] The implementation of the IMM methodology requires devising a special elemental filter for each mode of the system. In the present example, the modes of the system are given by all possible combinations of magnetometer fault indicator values, amounting to 2^4 modes. Thus, the IMM bank should consist of 16 elemental filters. Given each mode, the estimation problem for the corresponding mathematical model is nonlinear; hence, each elemental filter is a nonlinear filter, for example, an EKF or a UKF. In the present example, the UKF was used. The particular UKF implementation was chosen to be the recently presented unscented quaternion estimator (USQUE) of Ref. 17. The USQUE state vector was augmented to take into account the measurement error dynamics given by Eqs. (38).

It is obvious that the performance of the IMM estimator critically depends on the performance of its elemental filters; an unsatisfactory performance of the elemental filters would necessarily lead to unsatisfactory performance of the entire filter bank. Because one of the elemental filters of the IMM scheme corresponds to the fault-free case, this filter is first compared to the new RB–IMM/QPF scheme in the fault-free situation, before comparing the performance of the entire UKF-based IMM estimator to the RB–IMM/QPF estimator in the fault-prone scenario.

In the fault-free situation, the UKF-based IMM estimator reduces to the USQUE of Ref. 17. Similarly, in the fault-free case, the RB-IMM/QPF filter reduces to the QPF of Ref. 13. It is assumed that both algorithms have no a priori knowledge about the initial spacecraft attitude. Figure 1 presents the root mean square (RMS) attitude estimation errors of the QPF and USQUE, obtained based on 10,000 Monte Carlo runs. The attitude estimation error is defined as the rotation angle between the estimated and the true attitudes, that is,

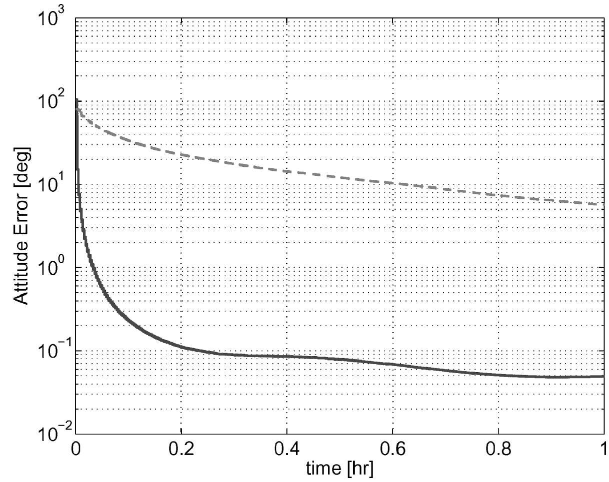

Fig. 1 RMS attitude estimation error in the fault-free scenario: ——, QPF and – – –, USQUE.

$$\Delta\varphi_k \triangleq 2\cos^{-1}(q_{4_k}\hat{q}_{4_{k|k}} + \varrho_k \cdot \hat{\varrho}_{k|k}) \tag{40}$$

where

$$\hat{q}_{k|k} = \begin{bmatrix} \hat{\varrho}_{k|k}^T & \hat{q}_{4_{k|k}} \end{bmatrix}^T \tag{41}$$

is the quaternion estimate. Figure 1 clearly demonstrates the superiority of the particle filtering approach over the approximate UKF approach. (Notice the ordinate logarithmic scale.) This result, which agrees well with the results reported in Ref. 13, is due to the strong nonlinearity in the system measurement equations. Because the USQUE plays the role of an elemental filter in the global UKF-based IMM scheme, and because other elemental filters in that scheme consist of the same fault-free filter when augmented by the fault states, it is obvious, then, that in the fault-prone scenario, when the fault probability is nonzero, the proposed RB–IMM/QPF scheme would be vastly superior to the UKF-based IMM approach.

Comparison to the Reversed R–B Approach

As already mentioned, another UKF-based approach is the reversed R–B method, presented in Ref. 15. According to this method, the continuously distributed states (in the present case, the attitude quaternion as well as the measurement biases) are estimated by a closed-form filter. The fault mode parameters are estimated by a PF.

To compare the RB–IMM/QPF to the reversed approach of Ref. 15, the latter filter is run with a PF employing 30 particles to approximate the distribution of the 4 binary fault indicators, whereas a UKF is used to estimate the state vector. This filter is termed RB–UKF/PF.

Figure 2 presents the rms attitude estimation errors of the RB-IMM/QPF and reversed R–B algorithms. (Notice the ordinate logarithmic scale.) The rms errors of the RB–IMM/QPF and the RB–UKF/PF are based on 6000 Monte Carlo runs. Note from Fig. 2 that the RB–IMM/QPF error is more than 20 times smaller than that of the RB–UKF/PF. The spikes in the RB–IMM/QPF rms error curve are due to the reinitialization logic implemented in the RB–IMM/QPF algorithm and are associated with the particle set dimension reduction stage. Because the filter is fully aware of the initialization procedure, this phenomenon can be alleviated, and moreover, an indicator of the temporary estimation vulnerability can be provided to the user during filter initializations.

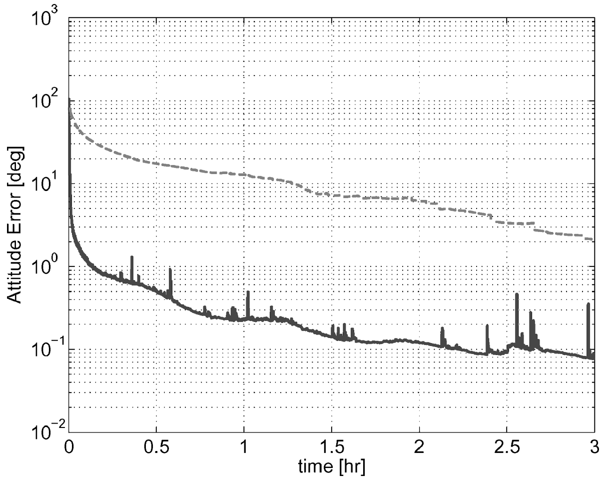

Fig. 2 RMS angular errors in the fault-prone situation: ——, RB–IMM/QPF and – – –, RB–UKF/PF.

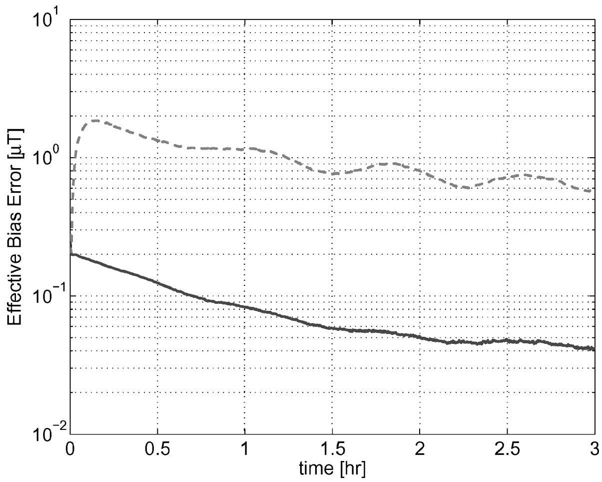

Fig. 3 Effective measurement bias errors in the fault-prone situation: ——, RB–IMM/QPF and – – –, RB–UKF/PF.

Figure 3 shows the time behavior of the root sum square of the components of the effective measurement bias rms estimation errors for the two compared filters. The effective biases are defined as

$$b_{\mathrm{eff}_k}^{(i)} \triangleq \gamma_k^{(i)} b_k^{(i)}, \qquad i = 1, 2, 3, 4 \tag{42}$$

One can see that, whereas the RB–IMM/QPF estimation error monotonically decreases with time, the estimation error associated with the RB–UKF/PF is unable to reach even its a priori value.

VI. Conclusions

This paper has addressed the problem of fault-tolerant particle filtering in highly nonlinear systems with fault-prone scalar measurement channels. As an alternative to the straightforward but computationally prohibitive state augmentation methodology, the R–B technique has been adopted in this work to reduce the number of particles. The filtering algorithm presented evaluates just the main state variables using a particle set, whereas the parameters of each measurement channel are estimated using a separate scalar IMM algorithm. This approach is reversed compared to the approach of another recently reported filter using the R–B methodology. The role reversal between the PF and the closed-form filter is significant in highly nonlinear systems because the approach taken herein applies no approximation to the nonlinear part of the system. Thus, the proposed filtering scheme enjoys increased accuracy and robustness relative to comparable existing algorithms.

A numerical study involving spacecraft attitude estimation using four fault-prone magnetometers is presented. The study compares the performance of the proposed filter to the conventional IMM approach (using the unscented Kalman filtering technique for its elemental filters) and to the reversed R–B approach whereby the system's mode variables are estimated using a PF and all other states are estimated via a UKF. The example clearly demonstrates the superiority of the proposed technique over both UKF-based alternatives. In particular, the study demonstrates the advantage of using the particle filtering methodology, relative to using the classical approach based on the IMM methodology.

References

[1]White, N. A., Maybeck, P. S., and DeVilbiss, S. L., "Detection of Interference/Jamming and Spoofing in a DGPS-Aided Inertial System," *IEEE Transactions on Aerospace and Electronic Systems*, Vol. AES-34, No. 4, 1998, pp. 1208–1217.

[2]Farrell, J., and Givargis, T., "Differential GPS Reference Station Algorithm—Design and Analysis," *IEEE Transactions on Control Systems Technology*, Vol. 8, No. 3, 2000, pp. 519–531.

[3]Wertz, J. R., *Spacecraft Attitude Determination and Control*, Reidel, Dordrecht, The Netherlands, 1978, pp. 198, 251.

[4]Tugnait, J. K., "Detection and Estimation for Abruptly Changing Systems," *Automatica*, Vol. 18, No. 5, 1982, pp. 607–615.

[5]Zhang, Y., and Li, R. X., "Detection and Diagnosis of Sensor and Actuator Failures Using IMM Estimator," *IEEE Transactions on Aerospace and Electronic Systems*, Vol. AES-34, No. 4, 1998, pp. 1293–1313.

[6]Caines, P. E., and Zhang, J.-F., "On the Adaptive Control of Jump Parameter Systems via Nonlinear Filtering," *SIAM Journal on Control and Optimization*, Vol. 33, No. 6, 1995, pp. 1758–1777.

[7]Ackerson, G. A., and Fu, K. S., "On State Estimation in Switching Environments," *IEEE Transactions on Automatic Control*, Vol. AC-15, No. 1, 1970, pp. 10–17.

[8]Costa, O. L. V., "Minimum Mean Square Error Estimator for Discrete-time Markovian Linear Systems," *IEEE Transactions on Automatic Control*, Vol. AC-39, No. 8, 1994, pp. 1685–1689.

[9]Blom, H. A. P., and Bar-Shalom, Y., "The Interacting Multiple Model Algorithm for Systems with Markovian Switching Coefficients," *IEEE Transactions on Automatic Control*, Vol. AC-33, No. 8, 1988, pp. 780–783.

[10]Anderson, B. D. O., and Moore, J. B., *Optimal Filtering*, Prentice–Hall, Englewood Cliffs, NJ, 1979, p. 195.

[11]Julier, S. J., Uhlmann, J. K., and Durrant-White, H. F., "A New Approach for Filtering Nonlinear Systems," *Proceedings of American Control Conference*, American Automatic Control Council, Evanston, IL, 1995, pp. 1628–1632.

[12]Doucet, A., de Freitas, N., and Gordon, N., *Sequential Monte Carlo Methods in Practice*, Springer-Verlag, New York, 2001, pp. 10, 21–25, 28, 91, 232, 251.

[13]Oshman, Y., and Carmi, A., "Estimating Attitude from Vector Observations Using a Genetic Algorithm-Embedded Quaternion Particle Filter," AIAA Paper 2004-5340, Aug. 2004.

[14]de Freitas, N., "Rao-Blackwellised Particle Filtering for Fault Diagnosis," *Proceedings of 2002 IEEE Aerospace Conference*, IEEE Publications, Piscataway, NJ, 2002, pp. 1767–1772.

[15]Hutter, F., and Dearden, R., "The Gaussian Particle Filter for Diagnosis of Non-Linear Systems," *Proceedings of the 5th IFAC Symposium on Fault Detection, Supervision and Safety of Technical Processes (SafeProcess-03)*, June 2003.

[16]Van Trees, H. L., *Detection, Estimation, and Modulation Theory, Part I*, Wiley, New York, 1968.

[17]Crassidis, J. L., and Markley, F. L., "Unscented Filtering for Spacecraft Attitude Estimation," *Journal of Guidance, Control, and Dynamics*, Vol. 26, No. 4, 2003, pp. 536–542.